Oxidation and spallation of FeCrAl alloys and thermal barrier coatings: in situ investigation under controlled temperature gradient

Julien Sniezewski, Yannick Le Maoult, Philippe Lours

Oxidation and spallation of FeCrAl alloys and thermal barrier coatings: *in situ* investigation under controlled temperature gradient

J. Sniezewski, Y. Le Maoult and P. Lours*
Université de Toulouse, Mines Albi, Institut Clement Ader, Campus Jarlard 81013 Albi Cedex 09, France
**E-mail: lours@enstimac.fr*

ABSTRACT

Alumina forming alloys and multi-material systems such as thermal barrier coatings (TBC) used for high temperature applications in aeronautical gas turbines are subject to severe thermo-mechanical loading. During service cycles, complex high stress is generated, resulting from the thermal variations that establish through the thickness of the multi-materials system. The occurrence of such thermal gradients may specifically provoke spallation and enhance the damage of the material surface. The cooling rate value is also an important factor influencing the material's life. In order to reproduce as close as possible those conditions of materials utilization, a dedicated, cyclic oxidation equipment is designed and implemented. It is able to impose a controlled and measurable thermal gradient through the material thickness and allows to monitor *in situ* the oxidation cycles using various optical means. Furthermore, the heating and cooling conditions are easily adjustable. This versatile real-time approach allows the identification and analysis of the spallation mechanisms for different micro-structural and time scales.

Preliminary results showing the impact of a thermal gradient as well as its magnitude on the propensity of an iron–chromium–aluminum ODS alloy and electron bean-physical vapour deposition TBC systems to spall upon thermal shock or thermal cycling are presented.

Keywords: oxidation, spallation, FeCrAl alloys, thermal barrier coatings, controlled temperature gradient

1. INTRODUCTION

Alumina forming alloys and superalloys coated with thermal barriers coatings (TBC) are used in industrial applications where superior properties at high temperature are required [1,2], namely mechanical strength, thermal insulation and oxidation resistance. Thermally grown oxides (TGO) that naturally develop on top of high-temperature alloys generally ensure a good protection against the environment provided their growth kinetics are slow and parabolic or sub-paprabolic, and their adhesion to the substrate is satisfactory [3]. In some cases, TBC are deposited, either by EB-PVD (electron beam–physical vapor deposition) or APS (atmospheric plasma spraying) to enhance the material performances by providing an additional thermal insulation. This both protects the alloys from the environments aggressiveness and increases drastically the service temperature as the (low thermal conductivity) TBC shields the alloy substrate by generating a strong thermal gradient between the hot gas and the turbine blades [4]. However, cyclic exposure at high temperature is prone to induce high surface stresses and may impair the integrity of the scale (TGO or TBC) by provoking detrimental spallation. For TBC systems failure of the TGO on the bond coat will also result in ceramic loss. This is particularly true in the case of complex transient temperature conditions as materials are exposed to severe through thickness thermal gradients [5,6] or during fast cooling. As a consequence, it is of primary importance to characterize and analyse the behaviour of such multi-materials in order to understand both the kinetics and the mechanisms of degradation [7,8]. This paper reports recent research aimed at designing and implementing a new, innovative experimental device to investigate the durability of TGO and TBC. Its specificity and originality lie in the possibility to impose a controlled thermal gradient to the investigated material while testing (to reproduce most industrial cases in aeronautics) and to monitor *in situ* the spallation mechanisms using optical means. Preliminary results showing the influence of (i) the magnitude of the thermal gradient, (ii) the substrate microstructure and mechanical properties and (iii) the scale thickness, on the overall scale damage are presented.

2. MATERIALS AND EXPERIMENTAL

Three types of multi-materials are investigated: the alumina forming alloy PM2000 ($Fe-20Cr-5.5Al-0.5Ti-0.5Y_2O_3$) (Figure 1a), a nickel base single crystal superalloy AM3, coated with β-(Ni, Pt)Al bond coat and 175 μm thick ZrO_2-

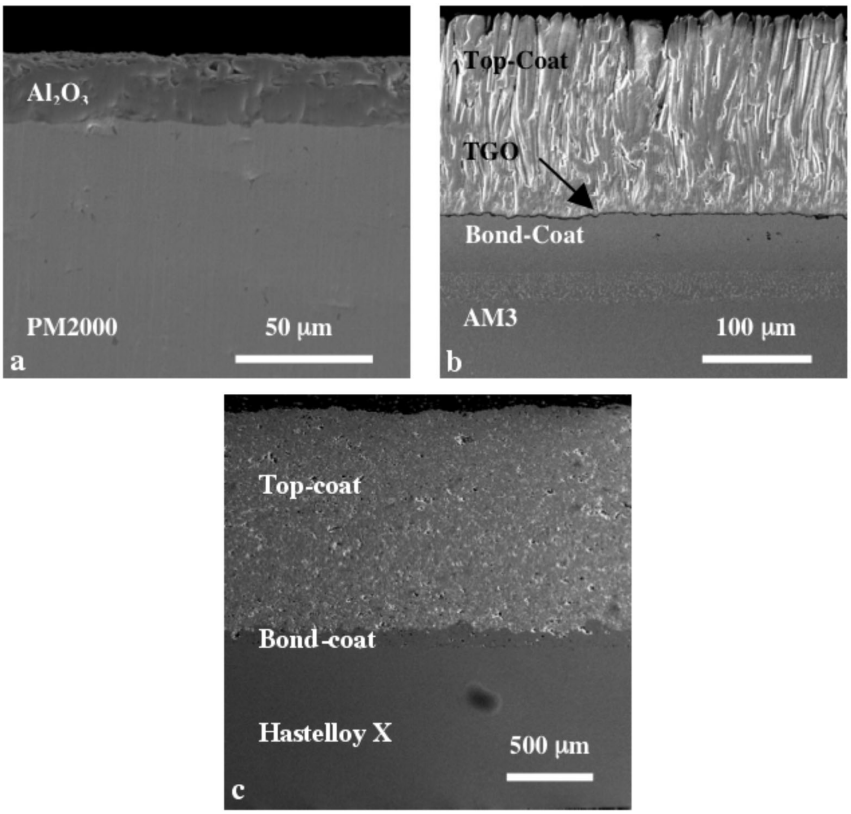

Figure 1 Cross-section SEM micrographs of oxidised PM2000 (384 h at 1300°C) (**a**), yittrium-stabilised-zirconia TBC deposited by EB-PVD (**b**), YSZ TBC deposited by APS (**c**).

8wt% Y_2O_3 top coat (yttrium stabilised zirconia (YSZ), deposited by EB-PVD) (Figure 1b), and IN738 superalloy coated with NiCrAlY bond coat and a 1000 μm YSZ top coat deposited by APS (Figure 1c). PM2000 is used in the shape of nearly square (22 mm by 25 mm), 6 mm thick specimens. They are ground down to 3 μm diamond paste. Coated AM3 are 2 mm thick discs with 10 mm diameter. Coated IN738 specimens are 2 mm thick discs with a 25 mm diameter. TBC specimens are oxidized in air at 1150°C according to the sequence of cycles shown in Figure 2 including successive 1 hour cycles. PM2000 specimens are held at 1300°C during 384 hours then cooled to room temperature at different rates to generate various thermal gradients through the material thickness. The *post-mortem* microstructural characterization is conducted using scanning-electron microscopy (SEM), energy-dispersive spectroscopy (EDS) and electron back scattering diffraction (EBSD). The analysis of images extracted from the various real-time video monitoring is performed using Aphelion software.

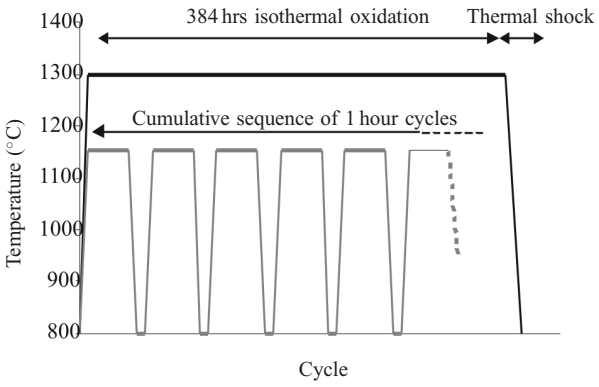

Figure 2 Oxidation cycles imposed to PM2000 alloy and cumulative 1 hour cycles imposed to thermal barriers coating systems.

3. DESIGN AND PERFORMANCES OF THE *IN SITU* THERMAL GRADIENT CONTROLLED CYCLIC OXIDATION TEST

In order to accurately reproduce at the laboratory scale, the thermal environment undergone by most material systems under industrial condition, it is necessary to design and implement a cyclic oxidation test able to impose a thermal gradient through the thickness of the investigated specimens. In addition, to view on a real-time basis the evolution of the oxidised and cycled surface, videometry is beneficially coupled such as to monitor *in situ* the damage mechanisms [9]. The test can be either used to study the cyclic oxidation behaviour of either high temperature (alumina or chromia forming alloys) or much more complex systems such as thermal barrier coatings.

3.1 General requirement

The experimental method is developed to satisfy the following general technical specifications:

(i) It is entirely automated, including the implementation of a computer-aided shuttle-furnace, whose motion on top and away from specimens, results in the required programmed thermal cycling.

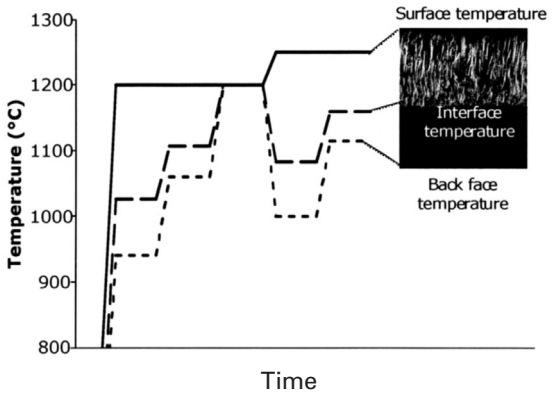

Figure 3 Thermal gradients across 170 μm thick EB-PVD YSZ and 2 mm thick AM3 substrate.

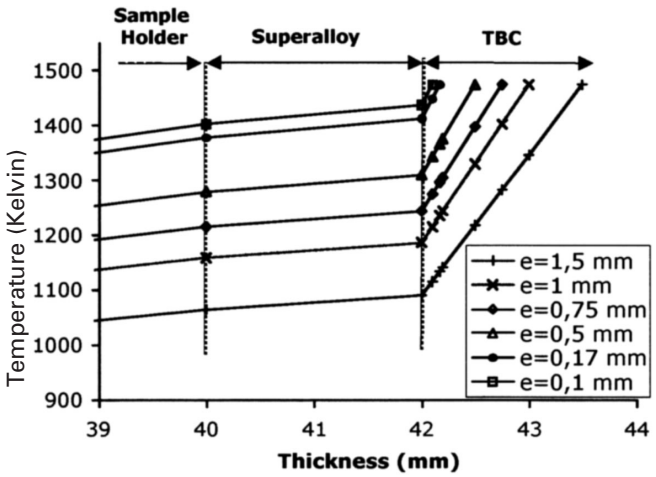

Figure 4 Calculated thermal gradient through hastelloy X substrate and APS TBC with various thicknesses.

(ii) It is versatile enough to cover a large range of possible programmable thermal cycles, by changing independently the cooling/heating rates, the holding time and temperature and the magnitude of the through thickness thermal gradient.

(iii) It can be instrumented with different kinds of cameras including high resolution, high-speed or IR cameras all with variable focal lengths, diaphragm aperture and viewing distance to increase or decrease the image resolution.

3.2 Thermal performances

The most innovative feature, and also the most difficult to achieve, of the cyclic oxidation test, is the implementation of a controlled and measurable thermal gradient across the material thickness. To do so, the heat flux crossing the back face of the specimen exposed to the furnace radiation, is continuously absorbed by the specimen holder. Such a heat exhaust is achieved using three complementary ways including: (i) the circulation of a coolant at the bottom of the specimen holder, (ii) the adjustment of the specimen-holder height by interposing ceramic discs in order to lower the overall thermal conductivity, and (iii) air flow during the cooling phase.

Figure 3 gives an example of how large the thermal gradient across a TBC can be. Three temperatures are given, namely the top surface temperature of the TBC measured with a pyrometer, the temperature on the back face of the substrate superalloy (single crystal AM3) measured with a thermocouple and the calculated temperature at the interface between the substrate and the EB-PVD YSZ (Femlab® software). During the heating phase, 600 to 1200 seconds are necessary to stabilize all the temperatures. This transient period depends on the total height of the sample-holder. All three temperatures can be changed, by varying the furnace power and/or the cooling capacity of the specimen-holder. For a top surface temperature of 1200°C (alternatively 1250°C), the back face temperature of the substrate can be adjusted from 940°C (alternatively 1083°C) to 1200°C (respectively 1250°C), leading to a gradient ranging between 173°C (alternatively 167°C) and 0°C (alternatively 0°C). It is generally assumed that an interface (substrate/TBC) temperature of 1000–1100°C corresponds more or less to the temperature suffered by aeronautical turbine blades. An upper temperature (1150°C) is typically used during laboratory cycles including a 10/15 minutes heating from room temperature to 1100–1150°C (heating rate about 1.3°C s^{-1}), a one hour high temperature holding and a 20 minutes cooling (cooling rate about 1°C s^{-1}). In such standard cycles, the whole specimen is held isothermally at high temperature, thus releasing any thermal stress induced by a thermal gradient. The cyclic oxidation test presented here is not only able to ensure such a gradient but it also allows the required interface temperature to be achieved and this temperature and consequently the gradient to be changed on purpose to apply more or less severe cycles.

Another interesting parameter that controls the interface temperature is, of course, the thickness of the coating. As indicated previously, several TBCs, deposited with different processes and characterized by various thicknesses, have been investigated. For given boundary conditions, including a top surface temperature of 1473 K (1200°C) and a sample-holder bottom end temperature of 293 K (20°C), an adiabatic stationary calculation is performed to estimate the gradient as a function of TBC thickness. Results for the APS-TBC thickness (from 100 to 1500 μm, the height of the stainless steel specimen-holder being 45 mm in all cases) are shown in Figure 4. The gradient ranges from 37 to 384°C respectively for the thinnest and the thickest TBC. Note that the gradient varies almost proportionally to the thickness of the YSZ.

3.3 Optical performance

A high-resolution CCD camera is used to monitor spallation events. The sensor is composed of a matrix with 1600 by 1200 pixels and can take 7.5 images per second in full resolution. To adjust the size of the investigated zone, the focal length can be varied from 45 to 200 mm. Beyond the specific benefit of monitoring *in situ* the spallation events, it is worth comparing the mass resolution of the technique to

Table 1 Mass resolution versus optical configuration

Sample configuration (200 μm thick TBC)	Pixel used/Pixel available	Mass resolution
Full screen $d_f = 45$ mm	$\alpha = 100\%$	0.917 μg
Three specimens with diameter 25 mm $d_f = 45$ mm	$\alpha = 51\%$	0.917 μg
Two rectangular specimens (21 × 26 mm) $d_f = 60$ mm	$\alpha = 65\%$	0.516 μg
Five specimens with diameter 10 mm $d_f = 52$ mm	$\alpha = 18\%$	0.687 μg
One specimen with diameter 10 mm $d_f = 200$ mm	$\alpha = 14\%$	0.046 μg

that of thermogravimetry, the standard technique commonly used to address oxidation and spallation behaviour. The resolution is directly related to the size of an elementary pixel and can be written as:

$$\Delta m = \left(\frac{d_s}{d_f}\right)^2 \delta x\, \delta y\, \xi_o \rho_o \quad (1)$$

where $d_s = 400$ mm is the distance from the camera to the specimen, d_f is the focal length of the camera, δ_x (4.4 μm) and δ_y (4.4 μm) are the sizes of a pixel for the camera used in the experiments, ξ_o and ρ_o are respectively the oxide or coating thickness and density.

Depending on the number and size of specimens viewed by the camera, the focal length can be changed to optimise the ratio of pixels used to form the image to the number of available pixels and/or the mass resolution. Examples are given in Table 1. Depending on the adopted configuration, the mass resolution ranges from 0.046 to 0.9 μg which is in any case far higher than the achievable resolution for thermogravimetry.

4. SPALLATION KINETICS AND MECHANISMS

4.1 Spallation of alumina thermally grown oxides

Literature reports that the severity of cooling during cyclic oxidation of high temperature alloys may strongly impact the propensity of the thermally grown oxide (TGO) to spall [9]. Depending on the cooling rate, which is straightforwardly controlled by the coolant in which the specimen-holder is immersed, a thermal gradient may establish or not through the thickness of the investigated material. To address the influence of the cooling rate and the thermal gradient on the spallation kinetics, various specimen-holder coolants are used: either air, ice or liquid nitrogen. For the three cases, the temperature gap between the top oxidised face and the back face of PM2000 specimens, initially held 384 hours at 1300°C to grow a *circa* 25 μm TGO, is plotted against the cooling time in Figure 5. Following an initial significantly short transient phase (~100 s) where the gradient drastically decreases, the temperature difference between the two specimen faces tends to level off, around (+50°C), (+15°C) and (0°) respectively for specimen-holder cooled in contact with liquid nitrogen, ice and air.

Generally speaking, in all cases, no spallation occurs during the transient phase where the temperature gradient still varies with the cooling time. Indeed, this phase being very short, the oxidised top surface of the alloy remains hot enough to release stress through creep deformation. In order to spall, the TGO must reach a temperature where no creep relaxation in the substrate is operative, which occurs during the stationary phase of cooling when the temperature gradient is constant.

Figure 6 shows the spallation kinetics, plotted for nine specimens of PM2000, each exposed 384 hours at 1300°C, strictly in the same oxidation condition and cooled down to room temperature in natural laboratory air. Though very similar in shape, the nine sigmoidal curves showing the instantaneous surface fraction of spall versus the cooling

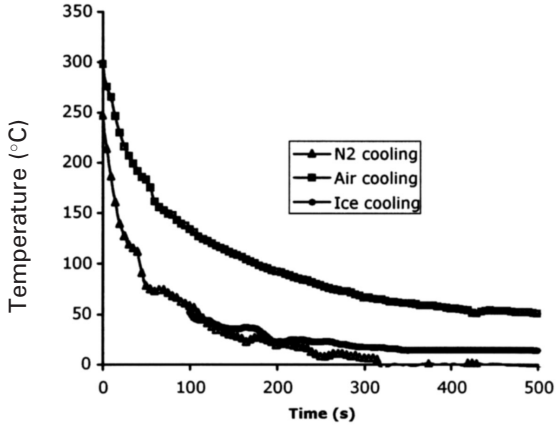

Figure 5 Specimen through-thickness thermal gradient for air, ice and liquid nitrogen cooled sample-holders (sample PM2000, with 25 μm thick alumina TGO).

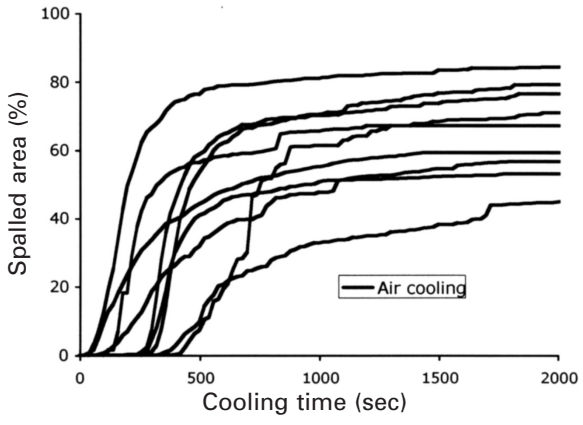

Figure 6 Spallation kinetics of PM2000 oxidised 384 h at 1300°C upon cooling in air-cooled sample-holder.

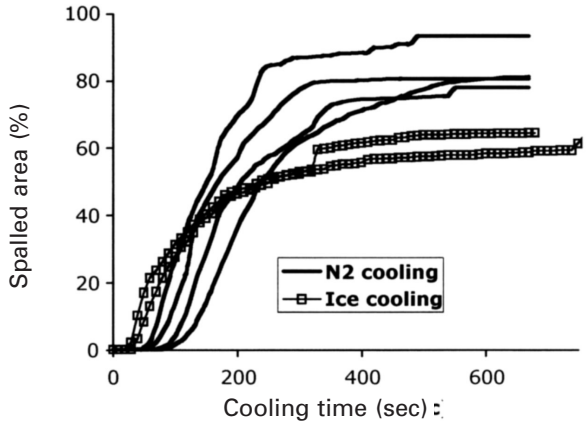

Figure 7 Spallation kinetics of PM2000 oxidised 384 hours at 1300°C upon cooling in ice-cooled and liquid nitrogen cooled sample-holder.

time, exhibit quite different characteristics. The critical time for spallation (or critical temperature), the spallation rates and the final total surface fraction of spall may significantly vary from one specimen to another. For different cooling conditions, namely using specimen-holder immersed in ice and liquid nitrogen, the spallation kinetics show the same tendency (Figure 7).

Both the mean values and the variances of the critical temperature for the onset of spallation T_c (top surface temperature for X% spallation), the spallation rate r (slope of the ascending part of the kinetics) and the final surface fraction of spall f are reported in Table 2. The table aims at comparing the influence on spallation of the different parameters related either to the material (*a*- the microstructure), the characteristics of the thermal shock (*b*- the thermal gradient) or the exposure time at high temperature (*c*- the oxide thickness).

As expected, the thickness of the oxide grown on substrates with a very close grain structure has a strong influence on the whole set of kinetics parameters. The overall propensity of the material to spall upon cooling is directly related to the thickness of the TGO. Similarly, the severity of cooling (and the associated magnitude of the temperature gradient through the specimen) is prone to enhance both the spallation rate r and the surface fraction of spall f. Also, it strongly shortens the incubation time for onset of spallation as the critical temperature for spallation T_c is the highest for the more severe cooling condition. Note however that compared to the strong impact of the liquid-nitrogen-cooling, no significant difference are noticeable between air-cooling and ice-cooling.

More surprisingly are the large differences exhibited by the nine specimens exposed at 1300°C and cooled under the same conditions. The thermal exposure and cooling procedure being rigorously identical, it is assumed that the significant spreading of the experimental results is essentially due to differences in microstructure from one specimen to another. This is quite interesting to note that the calculated variances in T_c, f and r induced by the difference in microstructure is comparable to that relative to the difference in oxide thickness or in cooling conditions. This unambiguously demonstrates the major role that the substrate microstructure has on the propensity of the alloy to damage through oxide spallation, following high-temperature exposure and subsequent cooling.

As indicated elsewhere [9], oxidised PM2000 alloy may spall following significantly different kinetics and mechanisms depending on the crystal orientation of the grains exposed to high temperature. Indeed, the alloy, designed for applications where superior creep resistance is required, has very large grains with high grain aspect ratio. Those elongated grains result from the overall mechanical alloying, extrusion and rolling process. They are highly textured and large enough to cover about one third of the specimen surface investigated as indicated in Figure 8a. The rolling direction (RD) is similar for all grains while the normal direction (ND) may vary slightly, depending on grain orientation, from crystal directions close to [111] to crystal directions close to [211]. This is illustrated in Figure 8b where the electron-back-scattering-diffraction (EBSD) response of the substrate is given.

Table 2 Comparative influence on spallation of the alloy substrate microstructure, the TGO thickness and the thermal gradient upon cooling of PM2000 oxidized at 1300°C [$\overline{\mathbf{T}}_c$ (*resp.* s_{Tc}), $\bar{\mathbf{f}}$ (*resp.* s_f) and r (*resp.* s_r) stand for the average values (*resp. the variance*) of the critical temperature for spallation, the total fraction of spall and the spallation rate]

		T_c (°C)		f (%)		$r = \Delta f/\Delta t$ (s^{-1})	
		$\overline{\mathbf{T}}_c$	s_{Tc}	$\bar{\mathbf{f}}$	s_f	$\bar{\mathbf{r}}$	s_r
(A) Microstructure	9 Tests	309	130	66	11	0.16	0.07
(B) Thermal gradient (°C)	Air	318		66		0.16	
	Ice	585		64		0.19	
			114		8.5		0.09
	N_2	525		83		0.36	
(C) Oxide thickness (μm) [after 8]	17	194		48		0.07	
	20	265		57		0.08	
	24	295	113	62	17	0.11	0.032
	36	500		94		0.15	

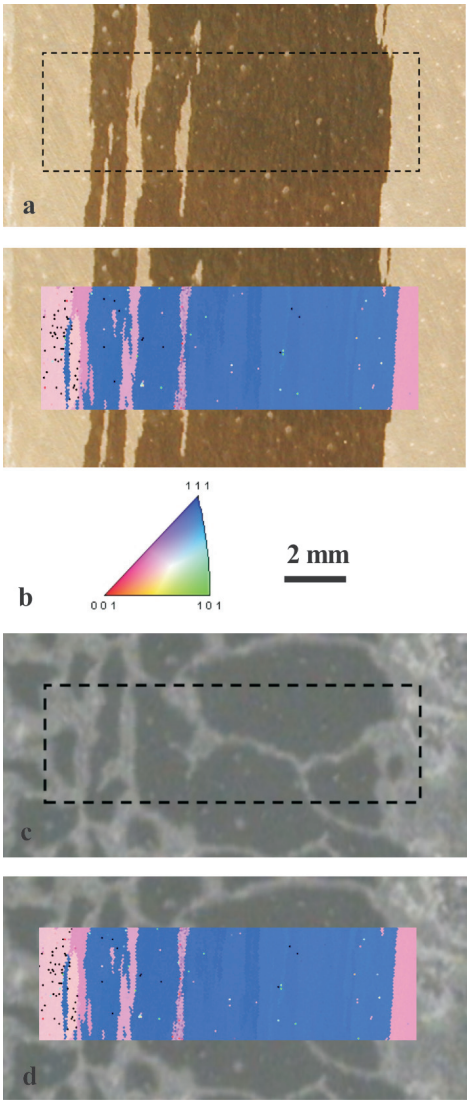

Figure 8 Grain structure of PM2000 (**a**), EBSD analysis (**b**), spallation figure following 384 h oxidation at 1300°C (**c**) and relation between the spall location and the crystal orientation of grains (**d**).

Figure 8c shows the alloy surface after oxidation and spallation. A thorough examination of spallation, occurring preferentially through the so-called buckling route [3,9,10], indicates that the oxide remains adherent in some parts (black contrast) while it has spalled off elsewhere (white contrast). Precisely, spallation preferentially occurs over those grains whose ND lies along crystal directions close to [211] as indicated by the superimposition of the EBDS and spallation figures in Figure 8d. Oxide grown on grains oriented along [111] is less subject to interfacial decohesion. It is assumed that depending on the crystal orientation of substrate grain, the epitaxial relation that establishes between the alloy and the oxide may differ impacting the adhesion properties of the TGO. Note, however, that degradation of the [111] surface may occur preferentially through the development of cracks that connect the various [211] spalled zones.

4.2 Spallation of thermal barrier coatings

Plotted in Figure 9 is the life evolution of the EB-PVD TBC studied as a function of the temperature generated at the interface between the superalloy and the YSZ during the exposure. These multi-materials systems are cyclically oxidised either:

- with a thermal gradient of about 90°C between the substrate top surface (interface with the top-coat) and the top face of the TBC; or
- with no thermal gradient (isothermal condition during holding time at high temperature).

The number of cycles to failure (N_R), varying exponentially with the interface temperature, has been arbitrarily chosen for a total surface fraction of spalling of 50%.

For the highest oxidation temperature, namely 1200°C, the presence or not of a thermal gradient does not result in any significant difference in N_R, *circa* 10 cycles. Surprisingly, for lower interface temperatures, TBC subject to thermal gradients are more resistant to spallation.

For test performed at an interface temperature of 1160°C, corresponding to the lowest oxidation temperature investigated, N_R increases drastically from 21 to 83 as the 90°C thermal gradient is established through the TBC thickness. This result, rather incoherent with the assumed higher thermomechanical stress induced by the temperature transient might be explained by the difference in the heating and the cooling rate. Indeed, the heating rate and the cooling rate are respectively lower and higher for the material tested with no thermal gradient. This both induces:

- a shorter cumulated holding time at high temperature, resulting in a lower thickness of the interfacial thermally grown alumina and correlatively an enhanced damage of the interface, and
- a higher thermomechanical stress generated upon cooling.

No significant difference is noted concerning the mechanisms of degradation of specimens oxidized with and without thermal gradient. Figure 10 shows the successive degradation and the failure morphology of an EB-PVD TBC exposed at 1180°C for 1 h cycle with no thermal gradient. Failure

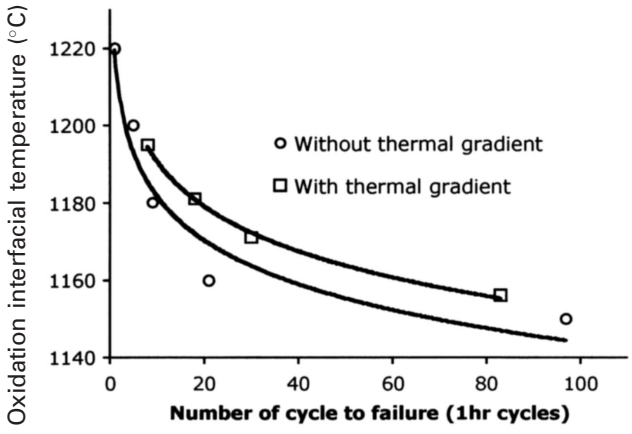

Figure 9 Life of TBC upon cyclic oxidation as the function of the temperature at the interface BC-TC.

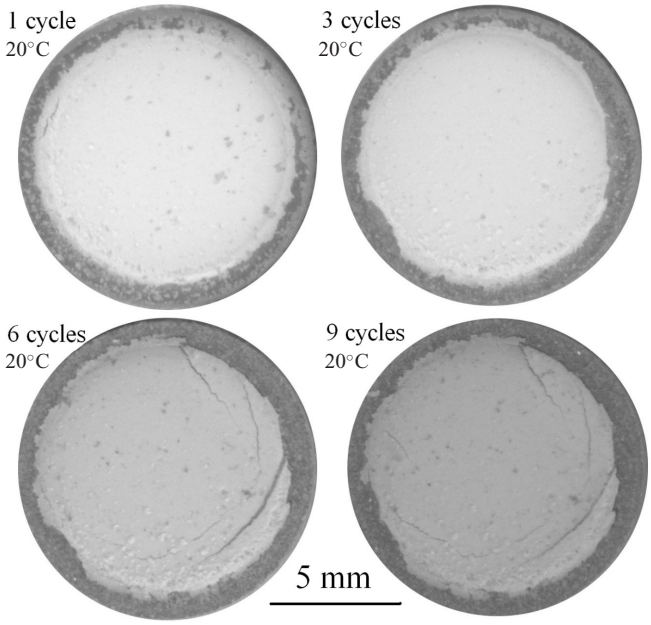

Figure 10 Spallation of EB-PVD TBC upon thermal cycles (total spallation for nine cycles).

initiates on specimen edges by developing cracks at temperature higher than 200°C. At lower temperature (100°C), cracks also initiate at the centre of the sample and small spalled particles are observed into the ceramic thickness. Cracks subsequently propagate at each cycle to provoke the complete spallation of the TBC following the ninth cycle. This full spallation occurs very abruptly (less than 0,13 s) at 90°C with an ejection of the TBC to some centimetres away from the sample. To some extent, this early degradation of the TBC might be a consequence of the high sulfur content of the AM3 substrate. Indeed, the diffusion and segregation of this detrimental element may dramatically impair the integrity of the interface.

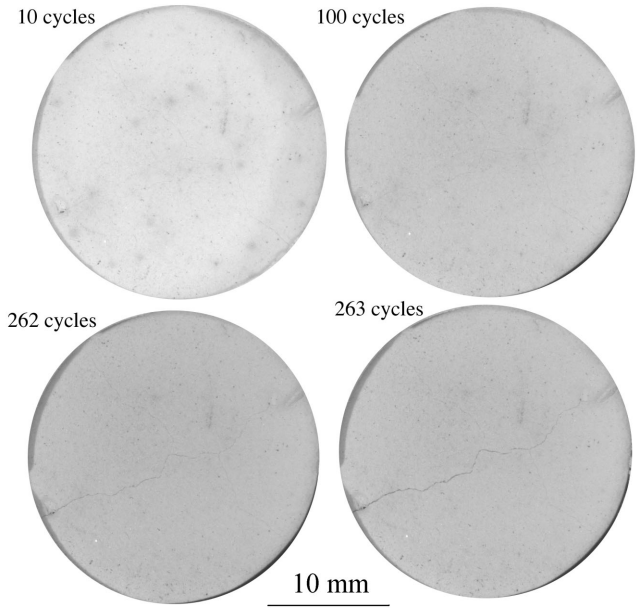

Figure 11 Spallation of APS TBC upon thermal cycles (total spallation for 263 cycles).

For thicker APS TBC, typically 1000 µm, the degradation is significantly delayed (Figure 11). Within those barriers, the through thickness thermal gradient is close to 250°C as a consequence of the high TBC thickness. Correlatively, for a given oxidation temperature (typically 1200°C in the present case), the temperature at the interface between the substrate and the coating is strongly decreased down to 950°C. Spallation proceeds according to a similar sequence of crack initiation and propagation resulting, after 263 cycles, in the complete delamination of the TBC. The higher resistance to spallation of high thickness APS TBC is a direct consequence of:

- the enhanced thermal insulation resulting in a lower interfacial temperature prone to limit the microstructural damage responsible for the degradation
- the lower creep resistance of the IN738 polycrystal resulting in a higher release of the thermomechanical stresses induced by the successive thermal cycles.

5. CONCLUSION

The design and implementation of a new automated cyclic oxidation test is presented. The specificities of the test consist in: (i) the precise control of the thermal gradient that establishes through the thickness of the investigated specimens to closely reproduce the condition of high temperature materials use, and (ii) the video recording of cooling sequences to address surface degradation on a real-time basis. Thermal and optical performances of the test are discussed and results obtained on TGO and TBC are presented.

For an alumina-forming FeCrAl alloy, the substrate microstructure as well as the magnitude of the thermal gradient, related to the cooling rate, have a strong impact on the propensity of the TGO to spall. In the case of TBC, behaviour differences are reported between low thickness EB-PVD YSZ that early degrade after nine 1-hour cycles, at an interface temperature of 1180°C and high thickness APS YSZ, more resistant to spallation as it lowers the interface temperatures to 950°C. This difference is due both to the difference in creep properties of the superalloy substrates and the difference of the temperature established at the interface between the substrate and the coating.

In addition, it is shown that the thermal cycling with a thermal gradient through the thickness of the EB-PVD TBC does not enhance the spallation of the system. Alhough surprising, this result is satisfactorily explained considering the precise profile of the thermal loading imposed to the materials. Namely, the characteristic of the heating and cooling rates as well as the total hot time favoured a better resistance to spallation of materials tested with a through thickness temperature gradient. Experiments are in progress to test EB-PVD TBC according to a thoroughly controlled thermal cycling identical for both types of conditions allowing to more accurately discriminate the impact of the thermal gradient and the impact of the thermal cycle characteristics.

ACKNOWLEDGEMENT

The authors gratefully acknowledge F. Crabos and A. Raffaitin (Turbomeca) and Professor J.R. Nicholls (University of Cranfield) for processing and providing thermal barrier coatings as well as J.Y. Perrin (CEMEF) for performing EBSD analysis. Part of this work was supported by ANR under contract Project ANR-CISBAT (ANR-2007-P2IC-001-01).

6. REFERENCES

[1] Schulz, U. *et al*. (2003) *Aerospace Sci. Technol*., **7**, 73.
[2] Evans, A.G. *et al*. (2001) *Prog. Mater. Sci*., **46**, 505–553.
[3] Evans, H.E. (1995) *Int. Mater. Rev.*, **40**, 1–40.
[4] Nicholls, J.R., Lawson, K.J., Johnstone, A. and Rickerby, D.S. (2007) *Surf. Coat. Technol*., **201**, 7905–7916.
[5] Evans, A.G. and Hutchinson, J.W. (2002) *Surf. Coat. Technol*., **151–152**, 383–391.
[6] Mao, W.G., Dai, C.Y., Zhou, Y.C. and Liu, Q.X. (2007) *Surf. Coat. Technol*., **201**, 6217–6227.
[7] Monceau, D. and Poquillon, D. (2004) *Oxidat. Met*., **61**, 143–163.
[8] Nychka, J.A. and Clarke, D.R. (2001) *Surf. Coat. Tech*., **146–147**, 110–116.
[9] Lours, P., Sniezewski, J., LeMaoult, Y. and Pieraggi, B. (2008) *Mater. Sci. Eng., A*, **480**(1–2), 40–48.
[10] Clarke, D.R., Tolpygo, V.K. and Gentleman, M. (2004) *Mater. Sci. Forum*, **461–464**, 621–630.